

2-бөлім**Раздел 2****Section 2****Қолданылмалы
математика****Прикладная
математика****Applied
Mathematics**

IRSTI 27.35.29

HFD method for large eddy simulation of MHD turbulence decay

Abdibekova A.U., al-Farabi Kazakh National University,
Almaty, Kazakhstan, +77029299933, E-mail: a.aigerim@gmail.com

Zhakebayev D.B., al-Farabi Kazakh National University,
Almaty, Kazakhstan, +77017537477, E-mail: daurjaz@mail.ru

This work deals with the modelling of the Magnetohydrodynamic (MHD) turbulence decay by hybrid finite-difference method (HFDM) combining two different numerical methods: finite-difference and spectral methods. The numerical algorithm of hybrid method solves the Navier-Stokes equations and equation for magnetic field by a finite-difference method in combination with cyclic penta-diagonal matrix, which yields fourth-order accuracy in space and second-order accuracy in time. The pressure Poisson equation is solved by the spectral method. For validation of the developed algorithm the classical problem of the 3-D Taylor and Green vortex flow is considered without considering the magnetic field, and the simulated time-dependent turbulence characteristics of this flow were found to be in excellent agreement with the corresponding analytical solution valid for short times. We also demonstrate that the developed efficient numerical algorithm can be used to simulate the magnetohydrodynamic turbulence decay at different magnetic Reynolds numbers.

Key words: Magnetohydrodynamics, Taylor-Green vortex problem, hybrid finite difference method, spectral method, turbulence decay.

**МГД турбуленттіліктің азғындауын үлкен құйындар әдіспен модельдеу үшін
гибридті ақырлы-айырымдылық әдісі**

Абдибекова А.У., әл-Фараби атындағы Қазақ ұлттық университеті,
Алматы, Қазақстан, +77029299933, email - a.aigerim@gmail.com

Жакебаев Д.Б., әл-Фараби атындағы Қазақ ұлттық университеті,
Алматы, Қазақстан, +77017537477, E-mail: daurjaz@mail.ru

Бұл мақала ақырлы айырымдылық және спектрлік екі сандық әдістерді біріктіретін гибриді ақырлы-айырымдылық әдіспен (ГААӘ) магнитогидродинамикалық (МГД) турбуленттіліктің азғындауын моделдеуіне арналған. Кеңістікте төртінші реттік және уақыт бойынша үшінші реттік дәлдігін беретін бес-диагональды циклдық матрицамен ақырлы –айырымдылық әдіс көмегімен Навье-Стокс теңдеуінің және магнит өріс теңдеуінің шешімдерінің негізінде гибриді әдісінің сандық алгоритмі құрылған. Қысымға арналған Пуассон теңдеуі спектрлік әдіспен шешіледі. Дамытылған алгоритмді тексеру үшін магниттік өрісті ескермейтін Тэйлор және Грин үш өлшемді құйынды ағынның классикалық мәселесін қарастырамыз, және модельдеу арқылы алынған турбулентті сипаттамалары қысқа мерзімді интервалдағы аналитикалық шешімнің нәтижелерімен жақсы келісім береді. Әр түрлі Рейнольдс сандарында магнитогидродинамикалық турбуленттіліктің азғындауын модельдеу үшін дамыған тиімді сандық алгоритм қолданылуы мүмкін.

Түйін сөздер: Магнитогидродинамика, Тейлор-Грин құйындылық мәселесі, соңғы айырымдық гибриді әдіс, спектральдық әдіс, турбуленттіліктің азғындауы.

**Метод крупных вихрей для моделирования вырождения МГД турбулентности
конечно-разностным гибридным методом**

Абдибекова А.У., Казахский национальный университет имени аль-Фараби,
Алматы, Казахстан, +77029299933, email - a.aigerim@gmail.com

Жакебаев Д.Б., Казахский национальный университет имени аль-Фараби,
Алматы, Казахстан, +77017537477, E-mail: daurjaz@mail.ru

Данная работа посвящена моделированию вырождению магнитогидродинамической (МГД) турбулентности конечно-разностным гибридным методом (КРГМ), сочетающейся из двух различных численных методов: конечно-разностный и спектральный. Разработан численный алгоритм гибридного метода на основе решения уравнения Навье-Стокса и уравнения для магнитного поля конечно-разностным методом в сочетании с циклической пятидиагональной матрицей, которая дает точность четвертого порядка по пространству и точность третьего порядка по времени. Уравнение Пуассона для давления решается спектральным методом. Для валидации разработанного алгоритма рассматривается классическая задача трехмерного вихревого потока Тейлора и Грина без учета магнитного поля, и полученные турбулентные характеристики при моделировании имеют отличное согласование с результатами аналитического решения на краткосрочном отрезке времени. Также показано, что разработанный эффективный численный алгоритм может быть использован для моделирования вырождения магнитогидродинамической турбулентности при различных числах Рейнольдса.

Ключевые слова: Магнитогидродинамика, вихревая задача Тейлора-Грина, конечно-разностный гибридный метод, спектральный метод, вырождение турбулентности.

1 Introduction

In the study of turbulent flows of particular interest is the simulation of cascade processes of turbulent energy transmission, large-scale and small-scale vorticity, and various turbulent laws are closely interacting with each other. Cascade processes determine the internal structure of flows and the mechanism of turbulent dissipation. A lot of work was devoted to the study and description of cascade turbulence models [15], [21] So far, cascade models are mainly used for the study of isotropic turbulence, but their capabilities are not limited. Therefore, it is very important to build cascade models and study with their help the properties of such complex turbulent flows as magnetohydrodynamic (MHD) turbulence.

2 Literature review

The problem of the magnetic field influence on turbulent flows was first raised by [2], who provided basic equations and an analytical solution for the movement of an electrically conducting fluid. The first numerical study of magnetohydrodynamic turbulence problem of the first type conducted by [19] at the magnetic number $Re_m \ll 1$. The numerical experiment of Schumann was the reflection of the idea of [16], who researched a homogeneous isotropic flow influenced by an applied external magnetic field. The modeling outlined in the publications of these scientists is performed using a spectral method, which is used as the basis for presenting a quantitative description of magnetic damping, the emergence of anisotropy, and the dependency of the results on the presence or the absence of a non-linear summand in the Navier-Stokes equation. The low performance of computing machines at that time did not permit the full solution of this problem. Later, a similar problem was researched by [9] and later by [24]. These authors presented the results of direct numerical modeling of large-scale structures in a periodic magnetic field, which reflected a change in the turbulence statistical parameters as a result of an imposed magnetic field influence. The contribution of these scientists in this area of expertise is determined by proving that the behavior of two- and three-dimensional structures varies substantially. A similar result was obtained by [22] in examining locally isotropic structures by the method of large eddies. The process of the magnetic field influence on a developed turbulence was examined by [7],[14], and [14]

demonstrated the possibility of using the quasi-stationary approximation for the solution of the second type problem and suggested to use quasi-linear approximations to solve the problem at $Re_m = 20$. The aim of this study is to study MHD turbulence flows that are weakly induced by a homogeneous external magnetic field by adapting the existing finite-difference and spectral methods to this particular problem.

For validation of the developed algorithm the classical problem of the 3-D Taylor and Green vortex flow is considered, and the simulated time-dependent turbulence characteristics of this flow were found to be in excellent agreement with the corresponding analytical solution valid for short times. The classical problem proposed by Taylor and Green [21] who considered a possibility of solving the Navier-Stokes equations analytically by a method for successive approximations, in order to describe three-dimensional turbulence evolution (specifically energy cascade and viscous dissipation) over time, with the resulting flow now known as the Taylor-Green vortex flow. Their work was motivated by the decay of three-dimensional turbulent flow produced in a wind tunnel, a fundamental process in turbulent flow, due to the grinding down of eddies, produced by nonlinearity of the Navier-Stokes equations. In their work the kinetic energy and its dissipation rate were determined analytically.

Taylor and Green's original analytical investigation is rigorous only for short times. To extend the understanding of the 3D Taylor-Green vortex flow, Brachet *et al* [5] solved the Taylor-Green vortex problem by two methods: numerical solution using the spectral method and power-series analysis in time. The resulting average kinetic energy and energy spectra at different flow Reynolds numbers were presented and compared. Later, in [6] three dimensional Navier-Stokes equations were numerically integrated with the periodic Taylor-Green initial condition. In this direct numerical simulation study the slope of energy spectrum was compared with Kolmogorov's $-5/3$ slope in the inertial subrange. Moreover, the compressible Navier-Stokes equations have also been applied to the Taylor-Green vortex problem using large-eddy simulation in [8] at different grid resolutions, and the time evolutions of the kinetic energy and its dissipation rate were compared at different grid resolutions.

3 Materials and methods

To evaluate the MHD turbulence decay is necessary to numerically simulate the change of all physical parameters over time at different magnetic Reynolds number. This work is devoted to study of self-excitation of magnetic field and the motion of the conducting fluid at the same time taking into account acting forces. The idea is to specify in the phase space of initial conditions for the velocity field and magnetic field, which satisfy the condition of continuity [23]. Given initial condition with the phase space is translated into physical space using a Fourier transform. The obtained of velocity field and magnetic field are used as initial conditions for the filtered MHD equations. Further is solved the unsteady three-dimensional equation of magnetohydrodynamics to simulate MHD turbulence decay.

3.1 Statement of the problem

The numerical modeling of MHD turbulence decay based on the large eddy simulation method depending on the conductive properties of the incompressible fluid is reviewed. The numerical modeling of the problem is performed based on solving non-stationary filtered magnetic

hydrodynamics equations in conjunction with the continuity equation in the Cartesian coordinate system in a non-dimensional form:

$$\left\{ \begin{array}{l} \frac{\partial(\bar{u}_i)}{\partial t} + \frac{\partial(\bar{u}_i \bar{u}_j)}{\partial x_j} = -\frac{\partial(\bar{p})}{\partial x_i} + \frac{1}{Re} \frac{\partial}{\partial x_j} \left(\frac{\partial(\bar{u}_i)}{\partial x_j} \right) - \frac{\partial(\tau_{ij}^u)}{\partial x_j} + A \frac{\partial}{\partial x_j} (\bar{H}_i \bar{H}_j), \\ \frac{\partial(\bar{u}_j)}{\partial x_j} = 0, \\ \frac{\partial(\bar{H}_i)}{\partial t} + \frac{\partial(\bar{u}_j \bar{H}_i)}{\partial x_j} - \frac{\partial(\bar{H}_j \bar{u}_i)}{\partial x_j} = \frac{1}{Re_m} \frac{\partial}{\partial x_j} \left(\frac{\partial(\bar{H}_i)}{\partial x_j} \right) - \frac{\partial(\tau_{ij}^H)}{\partial x_j}, \\ \frac{\partial(\bar{H}_j)}{\partial x_j} = 0, \\ \tau_{ij}^u = ((\overline{u_i u_j}) - (\bar{u}_i \bar{u}_j)) - ((\overline{H_i H_j}) - (\bar{H}_i \bar{H}_j)), \\ \tau_{ij}^H = ((\overline{u_i H_j}) - (\bar{u}_i \bar{H}_j)) - ((\overline{H_i u_j}) - (\bar{H}_i \bar{u}_j)), \end{array} \right. \quad (1)$$

where \bar{u}_i ($i = 1, 2, 3$) are the velocity components, $\bar{H}_1, \bar{H}_2, \bar{H}_3$ are the magnetic field strength components, $A = H^2/(4\pi\rho V^2) = \Pi/Re_m^2$ is the Alfvén number, H is the characteristic value of the magnetic field strength, V is the typical velocity, $\Pi = (V_A L/\nu_m)^2$ is a dimensionless value (on which the value Π depends in the equation for \bar{H}_i). If $\Pi \ll 1$, then $\partial\bar{H}_i/\partial t = 0$. The publication by [11] discussed in detail the physics of phenomena related to the ability to disregard the summand $\partial\bar{H}_i/\partial t$. $(V_A)^2 = H^2/4\pi\rho$ is the Alfvén velocity, $\bar{p} = p + \bar{H}^2 A/2$ is the full pressure, t is the time, $Re = LV/\nu$ is the Reynolds number, $Re_m = VL/\nu_m$ is the magnetic Reynolds number, L is the typical length, ν is the kinematic viscosity coefficient, ν_m is the magnetic viscosity coefficient, ρ is the density of electrically conducting incompressible fluid, and τ_{ij}^u, τ_{ij}^H is the subgrid-scale tensors responsible for small-scale structures to be modeled.

To model a subgrid-scale tensor, a viscosity model is presented as $\tau_{ij}^u = -2\nu_T \bar{S}_{ij}$, where $\nu_T = (C_S \Delta)^2 (2\bar{S}_{ij} \bar{S}_{ij})^{\frac{1}{2}}$ is the turbulent viscosity, $\bar{S}_{ij} = (\partial\bar{u}_i/\partial x_j + \partial\bar{u}_j/\partial x_i)/2$ is the deformation velocity tensor value. To model a magnetic subgrid-scale tensor, a viscosity model is used: $\tau_{ij}^H = -2\eta_t \bar{J}_{ij}$, where $\eta_t = (D_S \Delta)^2 (\bar{J}_{ij} \bar{J}_{ij})^{\frac{1}{2}}$ is the turbulent magnetic diffusion, the coefficients C_S, D_S are calculated for each defined time layer, and $\bar{J}_{ij} = (\partial\bar{H}_i/\partial x_j - \partial\bar{H}_j/\partial x_i)/2$ is the magnetic rotation tensor reviewed by [23].

Periodic boundary conditions are selected at all borders of the reviewed area of the velocity components and the magnetic field strength.

The initial values for each velocity component and strength are defined in the form of a function that depends on the wave numbers in the phase space:

$$u_i(k_i, 0) = k_i^{\frac{b-2}{2}} e^{-\frac{b}{4} \left(\frac{k_i}{k_{\max}}\right)^2}; \quad H_i(k_i, 0) = k_i^{\frac{b-2}{2}} e^{-\frac{b}{4} \left(\frac{k_i}{k_{\max}}\right)^2},$$

where \bar{u}_i is the one-dimensional velocity spectrum, $i = 1$ refers to the longitudinal spectrum, $i = 2$ and $i = 3$ refer to the transverse spectrum, \bar{H}_i is the one-dimensional magnetic field strength spectrum, m is the spectrum power, and k_1, k_2, k_3 are the wave numbers.

For this problem we selected a variational parameter b and the wave number k_{max} , which determine the type of turbulence. In figure 1 the parameter b varies when $k_{max} = 10$. For modeling homogeneous MHD turbulence can be set parameters k_{max} and b , which correspond to the experimental data [20].

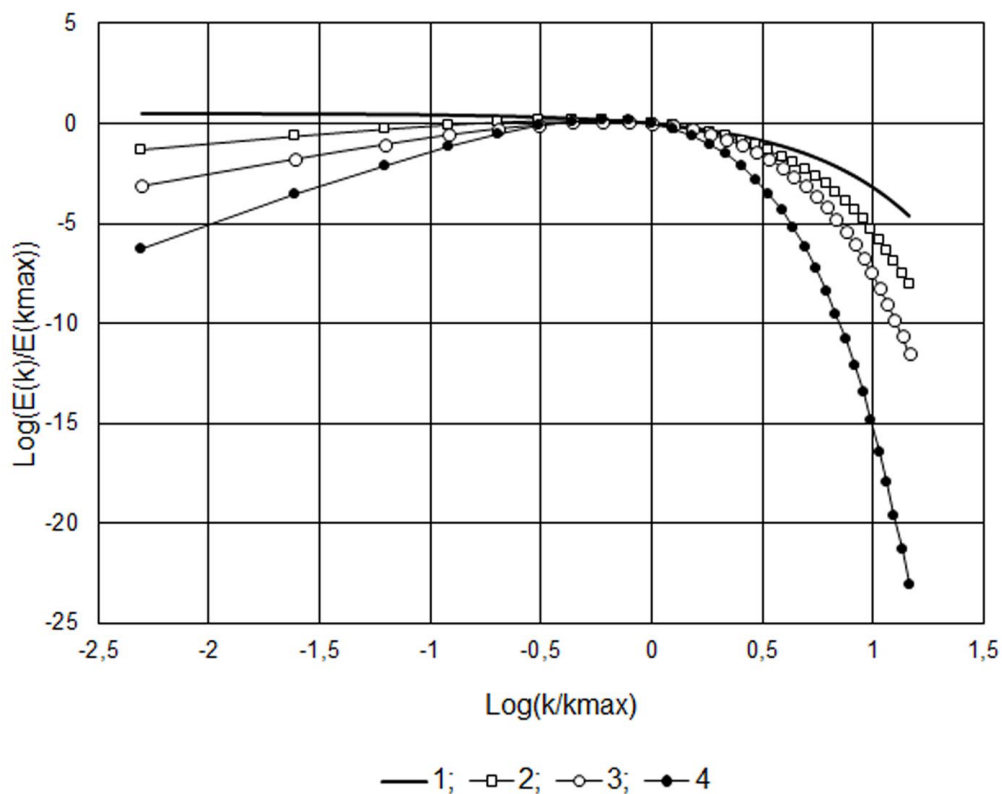


Figure 1: The equation of initial level turbulence, depending on the fixed wave number and the variational parameter b : 1) $b = 2$; 2) $b = 4$; 3) $b = 6$; 4) $b = 8$.

3.2 Numerical method

To solve the problem of homogeneous incompressible MHD turbulence, a scheme of splitting by physical parameters is used:

$$\text{I. } (\vec{u}^* - \vec{u}^n)/\Delta t = -(\vec{u}^n \nabla) \vec{u}^* + A \left(\vec{H}^n \nabla \right) \vec{H}^n + (1/Re) (\Delta \vec{u}^*) - \nabla \tau^u,$$

$$\text{II. } \Delta p = \nabla \vec{u}^* / \Delta t,$$

$$\text{III. } (\vec{u}^{n+1} - \vec{u}^*) / \Delta t = -\nabla p.$$

$$\text{IV. } \left(\vec{H}^{n+1} - \vec{H}^n \right) / \Delta t = -rot(\vec{u}^{n+1} \times \vec{H}^{n+1}) + (1/Re_m) \Delta \vec{H}^{n+1} - \nabla \tau^H$$

During the first stage, the Navier-Stokes equation is solved without the pressure consideration. For motion is solved, without taking pressure into account. For approximation of the convective and diffusion terms of the intermediate velocity field a finite-difference method in combination with cyclic penta-diagonal matrix is used [4], [18], which allowed to increase the order of accuracy in space. The intermediate velocity field is solved by using the Adams-Bashforth scheme in combination with a five-point sweep method. The numerical algorithm for the solution of incompressible MHD turbulence without taking into account large eddy simulation is considered at [1]. Let's consider the velocity component u_1 in the horizontal direction at the spatial location $(i + 1/2, j, k)$:

$$\frac{\partial u_1}{\partial t} + \frac{\partial(u_1 u_1)}{\partial x_1} + \frac{\partial(u_1 u_2)}{\partial x_2} + \frac{\partial(u_1 u_3)}{\partial x_3} = A \left(\frac{\partial(H_1 H_1)}{\partial x_1} + \frac{\partial(H_1 H_2)}{\partial x_2} + \frac{\partial(H_1 H_3)}{\partial x_3} \right) + \frac{1}{\text{Re}} \left(\frac{\partial^2 u_1}{\partial x_1^2} + \frac{\partial^2 u_1}{\partial x_2^2} + \frac{\partial^2 u_1}{\partial x_3^2} \right) - \left(\frac{\partial \tau_{11}^u}{\partial x_1} + \frac{\partial \tau_{12}^u}{\partial x_2} + \frac{\partial \tau_{13}^u}{\partial x_3} \right) \quad (2)$$

When using the explicit Adams-Bachfort scheme for convective terms and the implicit Crank-Nicholson scheme for viscous terms, equation (2) takes the form:

$$\begin{aligned} \widehat{u}_{1, i+\frac{1}{2}, j, k}^{n+1} - u_{1, i+\frac{1}{2}, j, k}^n &= -\frac{3\Delta t}{2} [hx]_{i+\frac{1}{2}, j, k}^n + \frac{\Delta t}{2} [hx]_{i+\frac{1}{2}, j, k}^{n-1} + \frac{\Delta t}{2} [ax]_{i+\frac{1}{2}, j, k}^n + \\ &+ \frac{\Delta t}{2} \frac{1}{\text{Re}} \cdot \left[\left(\frac{\partial^2 \widehat{u}_1}{\partial x_1^2} \right)_{i+\frac{1}{2}, j, k}^{n+1} + \left(\frac{\partial^2 \widehat{u}_1}{\partial x_2^2} \right)_{i+\frac{1}{2}, j, k}^{n+1} + \left(\frac{\partial^2 \widehat{u}_1}{\partial x_3^2} \right)_{i+\frac{1}{2}, j, k}^{n+1} \right] + \\ &+ \frac{3\Delta t}{2} [bx]_{i+\frac{1}{2}, j, k}^n - \frac{\Delta t}{2} [bx]_{i+\frac{1}{2}, j, k}^{n-1} - \frac{3\Delta t}{2} [\tau x]_{i+\frac{1}{2}, j, k}^n + \frac{\Delta t}{2} [\tau x]_{i+\frac{1}{2}, j, k}^{n-1}, \end{aligned} \quad (3)$$

where

$$[hx]_{i+\frac{1}{2}, j, k}^n = \left(\frac{\partial u_1 u_1}{\partial x_1} \right)_{i+\frac{1}{2}, j, k}^n + \left(\frac{\partial u_1 u_2}{\partial x_2} \right)_{i+\frac{1}{2}, j, k}^n + \left(\frac{\partial u_1 u_3}{\partial x_3} \right)_{i+\frac{1}{2}, j, k}^n,$$

$$[ax]_{i+\frac{1}{2}, j, k}^n = \frac{1}{\text{Re}} \cdot \left[\left(\frac{\partial^2 u_1}{\partial x_1^2} \right)_{i+\frac{1}{2}, j, k}^n + \left(\frac{\partial^2 u_1}{\partial x_2^2} \right)_{i+\frac{1}{2}, j, k}^n + \left(\frac{\partial^2 u_1}{\partial x_3^2} \right)_{i+\frac{1}{2}, j, k}^n \right]$$

$$[bx]_{i+\frac{1}{2}, j, k}^n = A \cdot \left[\left(\frac{\partial(H_1 H_1)}{\partial x_1} \right)_{i+\frac{1}{2}, j, k}^n + \left(\frac{\partial(H_1 H_2)}{\partial x_2} \right)_{i+\frac{1}{2}, j, k}^n + \left(\frac{\partial(H_1 H_3)}{\partial x_3} \right)_{i+\frac{1}{2}, j, k}^n \right]$$

$$[\tau x]_{i+\frac{1}{2}, j, k}^n = \left(\frac{\partial \tau_{11}^u}{\partial x_1} \right)_{i+\frac{1}{2}, j, k}^n + \left(\frac{\partial \tau_{12}^u}{\partial x_2} \right)_{i+\frac{1}{2}, j, k}^n + \left(\frac{\partial \tau_{13}^u}{\partial x_3} \right)_{i+\frac{1}{2}, j, k}^n$$

Discretization of convective terms look as [12]:

$$\begin{aligned} \left. \left(\frac{\partial u_1 u_1}{\partial x_1} \right) \right|_{i+\frac{1}{2},j,k} &= \frac{-(u_1^2)_{i+2,j,k} + 27(u_1^2)_{i+1,j,k} - 27(u_1^2)_{i,j,k} + (u_1^2)_{i-1,j,k}}{24\Delta x_1}, \\ \left. \left(\frac{\partial u_1 u_2}{\partial x_2} \right) \right|_{i+\frac{1}{2},j,k} &= \frac{(u_1 u_2)_{i+\frac{1}{2},j-\frac{3}{2},k} - 27(u_1 u_2)_{i+\frac{1}{2},j-\frac{1}{2},k}}{24\Delta x_2} + \\ &\quad + \frac{27(u_1 u_2)_{i+\frac{1}{2},j+\frac{1}{2},k} - (u_1 u_2)_{i+\frac{1}{2},j+\frac{3}{2},k}}{24\Delta x_2}, \\ \left. \left(\frac{\partial u_1 u_3}{\partial x_3} \right) \right|_{i+\frac{1}{2},j,k} &= \frac{(u_1 u_3)_{i+\frac{1}{2},j,k-\frac{3}{2}} - 27(u_1 u_3)_{i+\frac{1}{2},j,k-\frac{1}{2}}}{24\Delta x_3} + \\ &\quad + \frac{27(u_1 u_3)_{i+\frac{1}{2},j,k+\frac{1}{2}} - (u_1 u_3)_{i+\frac{1}{2},j,k+\frac{3}{2}}}{24\Delta x_3}, \end{aligned}$$

Discretization of diffusion terms look as:

$$\begin{aligned} \left. \left(\frac{\partial^2 u_1}{\partial x_1^2} \right) \right|_{i+\frac{1}{2},j,k} &= \frac{-(u_1)_{i+\frac{5}{2},j,k} + 16(u_1)_{i+\frac{3}{2},j,k} - 30(u_1)_{i+\frac{1}{2},j,k}}{12\Delta x_1^2} + \\ &\quad + \frac{16(u_1)_{i-\frac{1}{2},j,k} - (u_1)_{i-\frac{3}{2},j,k}}{12\Delta x_1^2}, \\ \left. \left(\frac{\partial^2 u_1}{\partial x_2^2} \right) \right|_{i+\frac{1}{2},j,k} &= \frac{-(u_1)_{i+\frac{1}{2},j+2,k} + 16(u_1)_{i+\frac{1}{2},j+1,k} - 30(u_1)_{i+\frac{1}{2},j,k}}{12\Delta x_2^2} + \\ &\quad + \frac{16(u_1)_{i+\frac{1}{2},j-1,k} - (u_1)_{i+\frac{1}{2},j-2,k}}{12\Delta x_2^2}, \\ \left. \left(\frac{\partial^2 u_1}{\partial x_3^2} \right) \right|_{i+\frac{1}{2},j,k} &= \frac{-(u_1)_{i+\frac{1}{2},j,k+2} + 16(u_1)_{i+\frac{1}{2},j,k+1} - 30(u_1)_{i+\frac{1}{2},j,k}}{12\Delta x_3^2} + \\ &\quad + \frac{16(u_1)_{i+\frac{1}{2},j,k-1} - (u_1)_{i+\frac{1}{2},j,k-2}}{12\Delta x_3^2}, \end{aligned}$$

where

$$\begin{aligned} (u_1 u_1)_{i,j,k} &= \left(\frac{-u_{1i+\frac{3}{2},j,k} + 9u_{1i+\frac{1}{2},j,k} + 9u_{1i-\frac{1}{2},j,k} - u_{1i-\frac{3}{2},j,k}}{16} \right)^2; \\ (u_1 u_2)_{i+\frac{1}{2},j+\frac{1}{2},k} &= \left(\frac{-u_{1i+\frac{1}{2},j+2,k} + 9u_{1i+\frac{1}{2},j+1,k} + 9u_{1i+\frac{1}{2},j,k} - u_{1i+\frac{1}{2},j-1,k}}{16} \right) \cdot \\ &\quad \cdot \left(\frac{-u_{2i+2,j+\frac{1}{2},k} + 9u_{2i+1,j+\frac{1}{2},k} + 9u_{2i,j+\frac{1}{2},k} - u_{2i-1,j+\frac{1}{2},k}}{16} \right); \\ (u_1 u_3)_{i+\frac{1}{2},j,k+\frac{1}{2}} &= \left(\frac{-u_{1i+\frac{1}{2},j,k+2} + 9u_{1i+\frac{1}{2},j,k+1} + 9u_{1i+\frac{1}{2},j,k} - u_{1i+\frac{1}{2},j,k-1}}{16} \right) \cdot \\ &\quad \cdot \left(\frac{-u_{3i+2,j,k+\frac{1}{2}} + 9u_{3i+1,j,k+\frac{1}{2}} + 9u_{3i,j,k+\frac{1}{2}} - u_{3i-1,j,k+\frac{1}{2}}}{16} \right); \end{aligned}$$

Discretization of magnetic field terms look as:

$$\begin{aligned} \left(\frac{\partial(H_1 H_1)}{\partial x_1} \right) \Big|_{i+\frac{1}{2},j,k} &= \frac{-(H_1^2)_{i+2,j,k} + 27(H_1^2)_{i+1,j,k}}{24\Delta x_1} + \\ &+ \frac{-27(H_1^2)_{i,j,k} + (H_1^2)_{i-1,j,k}}{24\Delta x_1}; \\ \left(\frac{\partial(H_1 H_2)}{\partial x_1} \right) \Big|_{i+\frac{1}{2},j,k} &= \frac{(H_1 H_2)_{i+\frac{1}{2},j-\frac{3}{2},k} - 27(H_1 H_2)_{i+\frac{1}{2},j-\frac{1}{2},k}}{24\Delta x_2} + \\ &+ \frac{27(H_1 H_2)_{i+\frac{1}{2},j+\frac{1}{2},k} - (H_1 H_2)_{i+\frac{1}{2},j+\frac{3}{2},k}}{24\Delta x_2}; \\ \left(\frac{\partial(H_1 H_3)}{\partial x_3} \right) \Big|_{i+\frac{1}{2},j,k} &= \frac{(H_1 H_3)_{i+\frac{1}{2},j,k-\frac{3}{2}} - 27(H_1 H_3)_{i+\frac{1}{2},j,k-\frac{1}{2}}}{24\Delta x_3} + \\ &+ \frac{27(H_1 H_3)_{i+\frac{1}{2},j,k+\frac{1}{2}} - (H_1 H_3)_{i+\frac{1}{2},j,k+\frac{3}{2}}}{24\Delta x_3}; \end{aligned}$$

The viscosity model and the subgrid-scale tensor are, respectively,

$$\begin{aligned} \tau_{11}^u &= -2\nu_T \cdot S_{11}, & S_{11} &= \frac{1}{2} \left(\frac{\partial u_1}{\partial x_1} + \frac{\partial u_1}{\partial x_1} \right) = 0, \\ \tau_{12}^u &= -2\nu_T \cdot S_{12}, & S_{12} &= \frac{1}{2} \left(\frac{\partial u_1}{\partial x_2} + \frac{\partial u_2}{\partial x_1} \right), \\ \tau_{13}^u &= -2\nu_T \cdot S_{13}, & S_{13} &= \frac{1}{2} \left(\frac{\partial u_1}{\partial x_3} + \frac{\partial u_3}{\partial x_1} \right), \end{aligned}$$

Discretization of the strength tensor terms look as:

$$\begin{aligned} \left(\frac{\partial(-\tau_{11}^u)}{\partial x_1} \right) \Big|_{i+\frac{1}{2},j,k} &= \frac{\partial}{\partial x_1} (2\nu_T \cdot S_{11}) = \frac{2}{\Delta x_1} \left[(\nu_T)_{i+\frac{1}{2},j,k} \cdot \left[\frac{(u_1)_{i+1,j,k} - (u_1)_{i,j,k}}{\Delta x_1} \right] + \right. \\ &\left. + (\nu_T)_{i-\frac{1}{2},j,k} \cdot \left[\frac{(u_1)_{i,j,k} - (u_1)_{i-1,j,k}}{\Delta x_1} \right] \right] = 0, \end{aligned}$$

$$\begin{aligned}
 \left(\frac{\partial(-\tau_{12}^u)}{\partial x_2} \right) \Big|_{i+\frac{1}{2},j,k} &= \frac{\partial}{\partial x_2} (2\nu_T \cdot S_{12}) = \\
 &= \frac{2}{2 \cdot \Delta x_2} \left[(\nu_T)_{i,j+\frac{1}{2},k} \cdot \left[\frac{(u_1)_{i,j+1,k} - (u_1)_{i,j,k}}{\Delta x_2} - \frac{(u_2)_{i+1,j,k} - (u_2)_{i,j,k}}{\Delta x_1} \right] + \right. \\
 &\quad \left. + (\nu_T)_{i,j-\frac{1}{2},k} \cdot \left[\frac{(u_1)_{i,j,k} - (u_1)_{i,j-1,k}}{\Delta x_2} - \frac{(u_2)_{i,j,k} - (u_2)_{i-1,j,k}}{\Delta x_1} \right] \right], \\
 \left(\frac{\partial(-\tau_{13}^u)}{\partial x_3} \right) \Big|_{i+\frac{1}{2},j,k} &= \frac{\partial}{\partial x_3} (2\nu_T \cdot S_{13}) = \\
 &= \frac{2}{2 \cdot \Delta x_3} \left[(\nu_T)_{i,j,k+\frac{1}{2}} \cdot \left[\frac{(u_1)_{i,j,k+1} - (u_1)_{i,j,k}}{\Delta x_3} - \frac{(u_3)_{i+1,j,k} - (u_3)_{i,j,k}}{\Delta x_1} \right] + \right. \\
 &\quad \left. + (\nu_T)_{i,j,k-\frac{1}{2}} \cdot \left[\frac{(u_1)_{i,j,k} - (u_1)_{i,j,k-1}}{\Delta x_3} - \frac{(u_3)_{i,j,k} - (u_3)_{i-1,j,k}}{\Delta x_1} \right] \right],
 \end{aligned}$$

Then the left hand side of equation (3) is denoted by $q_{i+\frac{1}{2}jk}$

$$q_{i+\frac{1}{2}jk} \equiv \widehat{u}_{1i+\frac{1}{2},j,k}^{n+1} - u_{1i+\frac{1}{2},j,k}^n. \tag{4}$$

We find $\widehat{u}_{1i+\frac{1}{2}jk}^{n+1}$ from equation (4)

$$\widehat{u}_{1i+\frac{1}{2},j,k}^{n+1} = q_{i+\frac{1}{2}jk} + u_{1i+\frac{1}{2},j,k}^n.$$

Replacing all $\widehat{u}_{1i+\frac{1}{2},j,k}^{n+1}$ from the equations (3) we obtain

$$\begin{aligned}
 q_{i+\frac{1}{2}jk} - \frac{\Delta t}{2} \cdot \frac{1}{\text{Re}} \cdot \left(\frac{\partial^2 q}{\partial x_1^2} \right)_{i+\frac{1}{2},j,k} - \frac{\Delta t}{2} \cdot \frac{1}{\text{Re}} \cdot \left(\frac{\partial^2 q}{\partial x_2^2} \right)_{i+\frac{1}{2},j,k} - \frac{\Delta t}{2} \cdot \frac{1}{\text{Re}} \cdot \left(\frac{\partial^2 q}{\partial x_3^2} \right)_{i+\frac{1}{2},j,k} &= \\
 &= -\frac{3\Delta t}{2} [hx]_{i+\frac{1}{2},j,k}^n + \frac{\Delta t}{2} [hx]_{i+\frac{1}{2},j,k}^{n-1} + \Delta t [ax]_{i+\frac{1}{2},j,k}^n + \\
 &\quad + \frac{3\Delta t}{2} [bx]_{i+\frac{1}{2},j,k}^n - \frac{\Delta t}{2} [bx]_{i+\frac{1}{2},j,k}^{n-1} - \frac{3\Delta t}{2} [\tau x]_{i+\frac{1}{2},j,k}^n + \frac{\Delta t}{2} [\tau x]_{i+\frac{1}{2},j,k}^{n-1},
 \end{aligned} \tag{5}$$

We can re-write equation (5) as

$$\left[1 - \frac{\Delta t}{2} \cdot \frac{1}{\text{Re}} \cdot \frac{\partial^2}{\partial x_1^2} - \frac{\Delta t}{2} \cdot \frac{1}{\text{Re}} \cdot \frac{\partial^2}{\partial x_2^2} - \frac{\Delta t}{2} \cdot \frac{1}{\text{Re}} \cdot \frac{\partial^2}{\partial x_3^2} \right] q_{i+\frac{1}{2}jk} = d_{i+\frac{1}{2},j,k}, \tag{6}$$

where

$$d_{i+\frac{1}{2}jk} = -\frac{3\Delta t}{2} [hx]_{i+\frac{1}{2},j,k}^n + \frac{\Delta t}{2} [hx]_{i+\frac{1}{2},j,k}^{n-1} + \Delta t [ax]_{i+\frac{1}{2},j,k}^n + \\ + \frac{3\Delta t}{2} [bx]_{i+\frac{1}{2},j,k}^n - \frac{\Delta t}{2} [bx]_{i+\frac{1}{2},j,k}^{n-1} - \frac{3\Delta t}{2} [\tau x]_{i+\frac{1}{2},j,k}^n + \frac{\Delta t}{2} [\tau x]_{i+\frac{1}{2},j,k}^{n-1},$$

Assuming that equation (6) has the second-order accuracy in time, we may solve the following equation instead:

$$\left[1 - \frac{\Delta t}{2} \cdot \frac{1}{\text{Re}} \frac{\partial^2}{\partial x_1^2}\right] \left[1 - \frac{\Delta t}{2} \frac{1}{\text{Re}} \cdot \frac{\partial^2}{\partial x_2^2}\right] \left[1 - \frac{\Delta t}{2} \cdot \frac{1}{\text{Re}} \frac{\partial^2}{\partial x_3^2}\right] q_{i+\frac{1}{2},j,k}^* = d_{i+\frac{1}{2},j,k}. \quad (7)$$

We can show that Equation (7) is an $O(\Delta t^4)$ approximation to equation (6) [13].

Equation (7) is a factorization approximation to equation (6), which allows each spatial direction to be treated sequentially. If we denote the solution to Equation (7) as $q_{i+\frac{1}{2}jk}^*$, by expanding Equation (7), subtracting equation (6) from it, and noting that $q_{i+\frac{1}{2}jk} \sim O(\Delta t^2)$, we obtain $(q_{i+\frac{1}{2}jk}^* - q_{i+\frac{1}{2}jk}) \sim O(\Delta t^4)$. Therefore, Equation (7) is actually an order $O(\Delta t^4)$ approximation to equation (6), rather than an order $O(\Delta t^3)$ approximation as stated in [13] without proof. Since the difference between $q_{i+\frac{1}{2}jk}^*$ and $q_{i+\frac{1}{2}jk}$ is of higher order, we shall return to the same notation and just use $q_{i+\frac{1}{2}jk}$.

To determine $q_{i+\frac{1}{2}jk}$, equation (7) is solved in 3 stages in sequence as follows:

$$\left[1 - \frac{\Delta t}{2} \cdot \frac{1}{\text{Re}} \cdot \frac{\partial^2}{\partial x_1^2}\right] A_{i+\frac{1}{2},j,k} = d_{i+\frac{1}{2},j,k}; \quad (8)$$

$$\left[1 - \frac{\Delta t}{2} \cdot \frac{1}{\text{Re}} \cdot \frac{\partial^2}{\partial x_2^2}\right] B_{i+\frac{1}{2},j,k} = A_{i+\frac{1}{2},j,k}; \quad (9)$$

$$\left[1 - \frac{\Delta t}{2} \cdot \frac{1}{\text{Re}} \cdot \frac{\partial^2}{\partial x_3^2}\right] q_{i+\frac{1}{2},j,k} = B_{i+\frac{1}{2},j,k}. \quad (10)$$

At the first stage, $A_{i+\frac{1}{2},j,k}$ is sought in the coordinate direction x_1 :

$$\left[1 - \frac{\Delta t}{2} \cdot \frac{1}{\text{Re}} \cdot \frac{\partial^2}{\partial x_1^2}\right] A_{i+\frac{1}{2},j,k} = d_{i+\frac{1}{2},j,k},$$

$$A_{i+\frac{1}{2},j,k} - \frac{\Delta t}{2} \cdot \frac{1}{\text{Re}} \cdot \left(\frac{\partial^2 A}{\partial x_1^2}\right)_{i+\frac{1}{2},j,k} = d_{i+\frac{1}{2},j,k},$$

$$A_{i+\frac{1}{2},j,k} - \frac{\Delta t}{2} \frac{1}{\text{Re}} \frac{-A_{i+\frac{5}{2},j,k} + 16A_{i+\frac{3}{2},j,k} - 30A_{i+\frac{1}{2},j,k} + 16A_{i-\frac{1}{2},j,k} - A_{i-\frac{3}{2},j,k}}{12\Delta x_1^2} = d_{i+\frac{1}{2},j,k}, \quad (11)$$

$$s_1 A_{i+\frac{5}{2},j,k} - 16s_1 A_{i+\frac{3}{2},j,k} + (1 + 30s_1) A_{i+\frac{1}{2},j,k} - 16s_1 A_{i-\frac{1}{2},j,k} + s_1 A_{i-\frac{3}{2},j,k} = d_{i+\frac{1}{2},j,k}, \quad (12)$$

where $s_1 = \frac{\Delta t}{24 \cdot \text{Re} \cdot \Delta x_1^2}$.

This equation (12) is solved by the cyclic penta-diagonal matrix method, which yields $A_{i+\frac{1}{2},j,k}$.

The same procedure is repeated next for the x_2 directions in the second stage, namely, $B_{i+\frac{1}{2},j,k}$ is obtained by solving equation (9), with the solution from the first stage as the coefficient on the right hand and the coefficient s_1 in the penta-diagonal matrix replaced by $s_2 = \frac{\Delta t}{24 \cdot \text{Re} \cdot \Delta x_2^2}$. Finally, in the third stage, $q_{i+\frac{1}{2},j,k}$ is solved through the similar penta-diagonal system shown in equation (10).

Once we have determined the value of $q_{i+\frac{1}{2},j,k}$, we find $\widehat{u}_{i+\frac{1}{2},j,k}^{n+1}$

$$\widehat{u}_{i+\frac{1}{2},j,k}^{n+1} = q_{i+\frac{1}{2},j,k} + u_{i+\frac{1}{2},j,k}^n.$$

The velocity components $\widehat{u}_{2,i,j+\frac{1}{2},k}^{n+1}$ and $\widehat{u}_{3,i,j,k+\frac{1}{2}}^{n+1}$ are solved in a similar manner.

3.3 Algorithm of solving the Poisson equation

In the second step, the pressure Poisson equation is solved, which ensures that the continuity equation is satisfied. The Poisson equation is transformed from the physical space into the spectral space by using a Fourier transform. The resulting intermediate velocity field does not satisfy the continuity equation. The final velocity field is obtained by adding to the intermediate field the term corresponding to the pressure gradient:

$$\begin{aligned} u_1^{n+1} &= \widehat{u}_1^{n+1} - \Delta t \frac{\partial p}{\partial x_1}; \\ u_2^{n+1} &= \widehat{u}_2^{n+1} - \Delta t \frac{\partial p}{\partial x_2}; \\ u_3^{n+1} &= \widehat{u}_3^{n+1} - \Delta t \frac{\partial p}{\partial x_3}. \end{aligned}$$

Substituting the continuity equation, we obtain the Poisson equation for the pressure field:

$$\frac{\partial^2 p}{\partial x_1^2} + \frac{\partial^2 p}{\partial x_2^2} + \frac{\partial^2 p}{\partial x_3^2} = \Delta t \left(\frac{\partial \widehat{u}_1^{n+1}}{\partial x_1} + \frac{\partial \widehat{u}_2^{n+1}}{\partial x_2} + \frac{\partial \widehat{u}_3^{n+1}}{\partial x_3} \right) \equiv F_{i,j,k},$$

where $F_{i,j,k}$ denotes the known right hand side of the Poisson equation, with each term approximated by an order $O(\Delta x^4)$ finite-difference approximation. For example, the first term in $F_{i,j,k}$ is approximated as

$$\Delta t \frac{\partial \widehat{u}_1^{n+1}}{\partial x_1} \Big|_{i+\frac{1}{2},j,k} = \Delta t \frac{\widehat{u}_{1i-\frac{3}{2},j,k}^{n+1} - 8\widehat{u}_{1i-\frac{1}{2},j,k}^{n+1} + 8\widehat{u}_{1i+\frac{3}{2},j,k}^{n+1} - \widehat{u}_{1i+\frac{5}{2},j,k}^{n+1}}{12\Delta x_1}.$$

To be consistent with the spatial accuracy in the first step, the left hand side of the above Poisson equation is discretized using 5-point scheme of $O(\Delta x^4)$ accuracy, as follows:

$$\begin{aligned} & \left[\frac{-P_{i+2,j,k} + 16P_{i+1,j,k} - 30P_{i,j,k} + 16P_{i-1,j,k} - P_{i-2,j,k}}{12\Delta x_1^2} \right] + \\ & + \left[\frac{-P_{i,j+2,k} + 16P_{i,j+1,k} - 30P_{i,j,k} + 16P_{i,j-1,k} - P_{i,j-2,k}}{12\Delta x_2^2} \right] + \\ & + \left[\frac{-P_{i,j,k+2} + 16P_{i,j,k+1} - 30P_{i,j,k} + 16P_{i,j,k-1} - P_{i,j,k-2}}{12\Delta x_3^2} \right] = F_{i,j,k}. \end{aligned} \quad (13)$$

Now we apply the three dimensional Fourier transform

$$\begin{aligned} P_{i,j,k} &= \frac{1}{N} \sum_{m=0}^{N_1-1} \sum_{n=0}^{N_2-1} \sum_{s=0}^{N_3-1} V_1^{im} V_2^{jn} V_3^{sk} \cdot \widehat{p}_{m,n,s}; \\ F_{i,j,k} &= \frac{1}{N} \sum_{m=0}^{N_1-1} \sum_{n=0}^{N_2-1} \sum_{s=0}^{N_3-1} V_1^{im} V_2^{jn} V_3^{sk} \cdot \widehat{f}_{m,n,s}. \end{aligned} \quad (14)$$

The inverse transforms are:

$$\begin{aligned} \widehat{p}_{m,n,s} &= \frac{1}{N} \sum_{i=0}^{N_1-1} \sum_{j=0}^{N_2-1} \sum_{k=0}^{N_3-1} V_1^{-im} V_2^{-jn} V_3^{-sk} \cdot P_{i,j,k}; \\ \widehat{f}_{m,n,s} &= \frac{1}{N} \sum_{i=0}^{N_1-1} \sum_{j=0}^{N_2-1} \sum_{k=0}^{N_3-1} V_1^{-im} V_2^{-jn} V_3^{-sk} \cdot F_{i,j,k}. \end{aligned} \quad (15)$$

where $N = N_1 \cdot N_2 \cdot N_3$, $V_1 = e^{i\left(\frac{2\pi}{N_1}\right)}$, $V_2 = e^{i\left(\frac{2\pi}{N_2}\right)}$, and $V_3 = e^{i\left(\frac{2\pi}{N_3}\right)}$.

Substituting equation (15) into equation (14), we obtain quickly the solution for the pressure field in the spectral space as

$$\widehat{p}_{m,n,s} = \frac{12\widehat{f}_{m,n,s}}{Q_1 + Q_2 + Q_3} \quad (16)$$

where

$$\begin{aligned} Q_1 &= \frac{1}{\Delta x_1^2} \left[-2 \cos \left(\frac{4\pi m}{N_1} \right) + 32 \cos \left(\frac{2\pi m}{N_1} \right) - 30 \right], \\ Q_2 &= \frac{1}{\Delta x_2^2} \left[-2 \cos \left(\frac{4\pi n}{N_2} \right) + 32 \cos \left(\frac{2\pi n}{N_2} \right) - 30 \right], \\ Q_3 &= \frac{1}{\Delta x_3^2} \left[-2 \cos \left(\frac{4\pi s}{N_3} \right) + 32 \cos \left(\frac{2\pi s}{N_3} \right) - 30 \right]. \end{aligned}$$

An inverse Fourier transform is then performed to obtain the pressure $P_{i,j,k}$ in the physical space. The obtained pressure field is then used at the third step to determine the final velocity field.

At the third stage, it is assumed that the transfer is carried out only by the pressure gradient, where the final velocity field is recalculated.

$$(\bar{u}^{n+1} - \bar{u}^*) / \Delta t = -\nabla p.$$

3.4 Algorithm for solving the equation of the magnetic field strength

Let us review equation (1) for the first component of the magnetic field strength in the horizontal direction at the spatial location $(i + 1/2, j, k)$:

$$\begin{aligned} & \frac{\partial H_1}{\partial t} + \frac{\partial}{\partial x_2} (u_2 H_1 - H_2 u_1) + \frac{\partial}{\partial x_3} (u_3 H_1 - H_3 u_1) - \\ & - \frac{1}{Re_m} \left[\frac{\partial^2 H_1}{\partial x_1^2} + \frac{\partial^2 H_1}{\partial x_2^2} + \frac{\partial^2 H_1}{\partial x_3^2} \right] = - \left(\frac{\partial \tau_{11}^H}{\partial x_1} + \frac{\partial \tau_{12}^H}{\partial x_2} + \frac{\partial \tau_{13}^H}{\partial x_3} \right). \end{aligned} \quad (17)$$

The strength of the magnetic field is found using the explicit Adams-Bachfort scheme for magnetic convective terms and the implicit Crank-Nicholson scheme for viscous terms, equation (17) takes the form:

$$\begin{aligned} \widehat{H}_{1i+\frac{1}{2},j,k}^{n+1} - H_{1i+\frac{1}{2},j,k}^n &= -\frac{3\Delta t}{2} [Hx]_{i+\frac{1}{2},j,k}^n + \frac{\Delta t}{2} [Hx]_{i+\frac{1}{2},j,k}^{n-1} + \frac{\Delta t}{2} [aHx]_{i+\frac{1}{2},j,k}^n + \\ & + \frac{\Delta t}{2} \frac{1}{Re} \cdot \left[\left(\frac{\partial^2 \widehat{H}_1}{\partial x_1^2} \right)_{i+\frac{1}{2},j,k}^{n+1} + \left(\frac{\partial^2 \widehat{H}_1}{\partial x_2^2} \right)_{i+\frac{1}{2},j,k}^{n+1} + \left(\frac{\partial^2 \widehat{H}_1}{\partial x_3^2} \right)_{i+\frac{1}{2},j,k}^{n+1} \right] - \\ & - \frac{3\Delta t}{2} [\tau Hx]_{i+\frac{1}{2},j,k}^n + \frac{\Delta t}{2} [\tau Hx]_{i+\frac{1}{2},j,k}^{n-1}, \end{aligned} \quad (18)$$

where

$$\begin{aligned} [Hx]_{i+\frac{1}{2},j,k}^n &= \left[\frac{\partial}{\partial x_2} (u_2 H_1 - H_2 u_1) \right]_{i+\frac{1}{2},j,k}^n + \left[\frac{\partial}{\partial x_3} (u_3 H_1 - H_3 u_1) \right]_{i+\frac{1}{2},j,k}^n \\ [aHx]_{i+\frac{1}{2},j,k}^n &= \frac{1}{Re_m} \cdot \left[\left(\frac{\partial^2 H_1}{\partial x_1^2} \right)_{i+\frac{1}{2},j,k}^n + \left(\frac{\partial^2 H_1}{\partial x_2^2} \right)_{i+\frac{1}{2},j,k}^n + \left(\frac{\partial^2 H_1}{\partial x_3^2} \right)_{i+\frac{1}{2},j,k}^n \right] \end{aligned}$$

$$[\tau Hx]_{i+\frac{1}{2},jk}^n = \left(\frac{\partial \tau_{11}^u}{\partial x_1} \right)_{i+\frac{1}{2},j,k}^n + \left(\frac{\partial \tau_{12}^u}{\partial x_2} \right)_{i+\frac{1}{2},j,k}^n + \left(\frac{\partial \tau_{13}^u}{\partial x_3} \right)_{i+\frac{1}{2},j,k}^n$$

Discretization of magnetic convective terms look as:

$$\begin{aligned} \left(\frac{\partial u_2 H_1}{\partial x_2} \right) \Big|_{i+\frac{1}{2},j,k} &= \frac{(u_2 H_1)_{i+\frac{1}{2},j-\frac{3}{2},k} - 27(u_2 H_1)_{i+\frac{1}{2},j-\frac{1}{2},k}}{24\Delta x_2} + \\ &+ \frac{27(u_2 H_1)_{i+\frac{1}{2},j+\frac{1}{2},k} - (u_2 H_1)_{i+\frac{1}{2},j+\frac{3}{2},k}}{24\Delta x_2}; \\ \left(\frac{\partial H_2 u_1}{\partial x_2} \right) \Big|_{i+\frac{1}{2},j,k} &= \frac{(H_2 u_1)_{i+\frac{1}{2},j-\frac{3}{2},k} - 27(H_2 u_1)_{i+\frac{1}{2},j-\frac{1}{2},k}}{24\Delta x_2} + \\ &+ \frac{27(H_2 u_1)_{i+\frac{1}{2},j+\frac{1}{2},k} - (H_2 u_1)_{i+\frac{1}{2},j+\frac{3}{2},k}}{24\Delta x_2}; \\ \left(\frac{\partial H_3 u_1}{\partial x_3} \right) \Big|_{i+\frac{1}{2},j,k} &= \frac{(H_3 u_1)_{i+\frac{1}{2},j,k-\frac{3}{2}} - 27(H_3 u_1)_{i+\frac{1}{2},j,k-\frac{1}{2}}}{24\Delta x_3} + \\ &+ \frac{27(H_3 u_1)_{i+\frac{1}{2},j,k+\frac{1}{2}} - (H_3 u_1)_{i+\frac{1}{2},j,k+\frac{3}{2}}}{24\Delta x_3}; \\ \left(\frac{\partial u_3 H_1}{\partial x_3} \right) \Big|_{i+\frac{1}{2},j,k} &= \frac{(u_3 H_1)_{i+\frac{1}{2},j,k-\frac{3}{2}} - 27(u_3 H_1)_{i+\frac{1}{2},j,k-\frac{1}{2}}}{24\Delta x_3} + \\ &+ \frac{27(u_3 H_1)_{i+\frac{1}{2},j,k+\frac{1}{2}} - (u_3 H_1)_{i+\frac{1}{2},j,k+\frac{3}{2}}}{24\Delta x_3}; \end{aligned}$$

Discretization of magnetic diffusion terms look as:

$$\begin{aligned} \left(\frac{\partial^2 H_1}{\partial x_1^2} \right) \Big|_{i+\frac{1}{2},j,k} &= \frac{-(H_1)_{i+\frac{5}{2},j,k} + 16(H_1)_{i+\frac{3}{2},j,k} - 30(H_1)_{i+\frac{1}{2},j,k}}{12\Delta x_1^2} + \\ &+ \frac{16(H_1)_{i-\frac{1}{2},j,k} - (H_1)_{i-\frac{3}{2},j,k}}{12\Delta x_1^2}; \\ \left(\frac{\partial^2 H_1}{\partial x_2^2} \right) \Big|_{i+\frac{1}{2},j,k} &= \frac{-(H_1)_{i+\frac{1}{2},j+2,k} + 16(H_1)_{i+\frac{1}{2},j+1,k} - 30(H_1)_{i+\frac{1}{2},j,k}}{12\Delta x_2^2} + \\ &+ \frac{16(H_1)_{i+\frac{1}{2},j-1,k} - (H_1)_{i+\frac{1}{2},j-2,k}}{12\Delta x_2^2}; \\ \left(\frac{\partial^2 H_1}{\partial x_3^2} \right) \Big|_{i+\frac{1}{2},j,k} &= \frac{-(H_1)_{i+\frac{1}{2},j,k+2} + 16(H_1)_{i+\frac{1}{2},j,k+1} - 30(H_1)_{i+\frac{1}{2},j,k}}{12\Delta x_3^2} + \\ &+ \frac{16(H_1)_{i+\frac{1}{2},j,k-1} - (H_1)_{i+\frac{1}{2},j,k-2}}{12\Delta x_3^2}, \end{aligned}$$

where

$$\begin{aligned}
 (u_2 H_1)_{i+\frac{1}{2},j+\frac{1}{2},k} &= \left(\frac{-u_{2i+2,j+\frac{1}{2},k} + 9u_{2i+1,j+\frac{1}{2},k} + 9u_{2i,j+\frac{1}{2},k} - u_{2i-1,j+\frac{1}{2},k}}{16} \right) \cdot \\
 &\cdot \left(\frac{-H_{1i+\frac{1}{2},j+2,k} + 9H_{1i+\frac{1}{2},j+1,k} + 9H_{1i+\frac{1}{2},j,k} - H_{1i+\frac{1}{2},j-1,k}}{16} \right); \\
 (H_2 u_1)_{i+\frac{1}{2},j+\frac{1}{2},k} &= \left(\frac{-H_{2i+2,j+\frac{1}{2},k} + 9H_{2i+1,j+\frac{1}{2},k} + 9H_{2i,j+\frac{1}{2},k} - H_{2i-1,j+\frac{1}{2},k}}{16} \right) \cdot \\
 &\cdot \left(\frac{-u_{1i+\frac{1}{2},j+2,k} + 9u_{1i+\frac{1}{2},j+1,k} + 9u_{1i+\frac{1}{2},j,k} - u_{1i+\frac{1}{2},j-1,k}}{16} \right); \\
 (u_3 H_1)_{i+\frac{1}{2},j,k+\frac{1}{2}} &= \left(\frac{-u_{3i+2,j,k+\frac{1}{2}} + 9u_{3i+1,j,k+\frac{1}{2}} + 9u_{3i,j,k+\frac{1}{2}} - u_{3i-1,j,k+\frac{1}{2}}}{16} \right) \cdot \\
 &\cdot \left(\frac{-H_{1i+\frac{1}{2},j,k+2} + 9H_{1i+\frac{1}{2},j,k+1} + 9H_{1i+\frac{1}{2},j,k} - H_{1i+\frac{1}{2},j,k-1}}{16} \right); \\
 (H_3 u_1)_{i+\frac{1}{2},j,k+\frac{1}{2}} &= \left(\frac{-H_{3i+2,j,k+\frac{1}{2}} + 9H_{3i+1,j,k+\frac{1}{2}} + 9H_{3i,j,k+\frac{1}{2}} - H_{3i-1,j,k+\frac{1}{2}}}{16} \right) \cdot \\
 &\cdot \left(\frac{-u_{1i+\frac{1}{2},j,k+2} + 9u_{1i+\frac{1}{2},j,k+1} + 9u_{1i+\frac{1}{2},j,k} - u_{1i+\frac{1}{2},j,k-1}}{16} \right);
 \end{aligned}$$

The viscosity model and the magnetic rotation tensor are, respectively,

$$\begin{aligned}
 \tau_{11}^H &= -2\eta_t \cdot J_{11}, & J_{11} &= \frac{1}{2} \left(\frac{\partial H_1}{\partial x_1} - \frac{\partial H_1}{\partial x_1} \right) = 0, \\
 \tau_{12}^H &= -2\eta_t \cdot J_{12}, & J_{12} &= \frac{1}{2} \left(\frac{\partial H_1}{\partial x_2} - \frac{\partial H_2}{\partial x_1} \right), \\
 \tau_{13}^H &= -2\eta_t \cdot J_{13}, & J_{13} &= \frac{1}{2} \left(\frac{\partial H_1}{\partial x_3} - \frac{\partial H_3}{\partial x_1} \right),
 \end{aligned}$$

The discretization of the magnetic rotation tensor terms look as:

$$\begin{aligned}
 \frac{\partial}{\partial x_1} (-\tau_{11}^H) &= 0, \\
 \frac{\partial}{\partial x_2} (-\tau_{12}^H) &= \frac{\partial}{\partial x_2} (2\eta_t \cdot J_{12}) = \\
 &= \frac{2}{2 \cdot \Delta x_2} \left[(\eta_t)_{i,j+\frac{1}{2},k} \cdot \left[\frac{(H_1)_{i,j+1,k} - (H_1)_{i,j,k}}{\Delta x_2} - \frac{(H_2)_{i+1,j,k} - (H_2)_{i,j,k}}{\Delta x_1} \right] - \right. \\
 &\left. - (\eta_t)_{i,j-\frac{1}{2},k} \cdot \left[\frac{(H_1)_{i,j,k} - (H_1)_{i,j-1,k}}{\Delta x_2} - \frac{(H_2)_{i,j,k} - (H_2)_{i-1,j,k}}{\Delta x_1} \right] \right],
 \end{aligned}$$

$$\begin{aligned} \frac{\partial}{\partial x_3} (-\tau_{13}^H) &= \frac{\partial}{\partial x_3} (2\eta_t \cdot J_{13}) = \\ &= \frac{2}{2 \cdot \Delta x_3} \left[(\eta_t)_{i,j,k+\frac{1}{2}} \cdot \left[\frac{(H_1)_{i,j,k+1} - (H_1)_{i,j,k}}{\Delta x_3} - \frac{(H_3)_{i+1,j,k} - (H_3)_{i,j,k}}{\Delta x_1} \right] - \right. \\ &\quad \left. - (\eta_t)_{i,j,k-\frac{1}{2}} \cdot \left[\frac{(H_1)_{i,j,k} - (H_1)_{i,j,k-1}}{\Delta x_3} - \frac{(H_3)_{i,j,k} - (H_3)_{i-1,j,k}}{\Delta x_1} \right] \right], \end{aligned}$$

The equation is solved by the similar penta-diagonal system shown in section II and is found to be $(H_1)_{i,j,k}^{n+\frac{1}{3}}$.

$(H_1)_{i,j,k}^{n+\frac{2}{3}}$, $(H_1)_{i,j,k}^{n+1}$ components of the magnetic field strength are defined in a similar way. Thus, all the components of the magnetic field strength determined this way.

3.5 Definition of homogeneous MHD turbulence characteristics

To identify turbulent characteristics in the physical space, it is necessary to average different values in volume. The averaged values will be used to find the turbulent characteristics. The procedure for calculating the turbulent characteristics is similar to the one specified in papers by [17] and [3]. The value averaged along the entire calculated area is calculated by the following formula:

$$\langle u_i \rangle = \frac{1}{N_1 N_2 N_3} \sum_{n=1}^{N_1} \sum_{m=1}^{N_2} \sum_{q=1}^{N_3} (\bar{u}_i)_{n,m,q}.$$

$$\langle H_i \rangle = \frac{1}{N_1 N_2 N_3} \sum_{n=1}^{N_1} \sum_{m=1}^{N_2} \sum_{q=1}^{N_3} (\bar{H}_i)_{n,m,q}$$

$$\langle u_1^2 \rangle = \langle u_1(x, y, z, t) \cdot u_1(x, y, z, t) \rangle,$$

$$\langle u_2^2 \rangle = \langle u_2(x, y, z, t) \cdot u_2(x, y, z, t) \rangle,$$

$$\langle u_3^2 \rangle = \langle u_3(x, y, z, t) \cdot u_3(x, y, z, t) \rangle.$$

The microscale length is determined by the following ratio:

$$\lambda_f = \left\{ \frac{2}{-f''(0)} \right\}^{1/2}, \quad \lambda_g = \left\{ \frac{2}{g''(0)} \right\}^{1/2}.$$

The integral scale is expressed as

$$\Lambda_f(t) = \int_0^{L/2} f(r, t) dr, \quad \Lambda_g(t) = \int_0^{L/2} g(r, t) dr.$$

The dissipation rate is calculated by the following formula:

$$\begin{aligned} \epsilon = \langle 2\nu S_{ij} S_{ij} \rangle = & 2\nu \left[\left\langle \left(\frac{\partial u_1}{\partial x_1} \right)^2 \right\rangle + \left\langle \left(\frac{\partial u_2}{\partial x_2} \right)^2 \right\rangle + \left\langle \left(\frac{\partial u_3}{\partial x_3} \right)^2 \right\rangle \right] + \\ & + 2\nu \left[\frac{1}{2} \left\langle \left(\frac{\partial u_1}{\partial x_2} + \frac{\partial u_2}{\partial x_1} \right)^2 \right\rangle + \frac{1}{2} \left\langle \left(\frac{\partial u_1}{\partial x_3} + \frac{\partial u_3}{\partial x_1} \right)^2 \right\rangle + \frac{1}{2} \left\langle \left(\frac{\partial u_2}{\partial x_3} + \frac{\partial u_3}{\partial x_2} \right)^2 \right\rangle \right] \end{aligned}$$

The turbulent kinematic energy is found in the following way: The turbulent kinetic and magnetic energy are, respectively,

$$E_{ku} = \frac{1}{2} (\langle u_1 \rangle^2 + \langle u_2 \rangle^2 + \langle u_3 \rangle^2) = \frac{3}{2} \langle u_1^2 \rangle,$$

$$E_{kh} = \frac{1}{2} (\langle H_1 \rangle^2 + \langle H_2 \rangle^2 + \langle H_3 \rangle^2) = \frac{3}{2} \langle H_1^2 \rangle.$$

Velocity derivative skewness is defined in the following form:

$$S(t) = \frac{\left\langle \frac{1}{3} \left[\left(\frac{\partial u_1}{\partial x_1} \right)^3 + \left(\frac{\partial u_2}{\partial x_2} \right)^3 + \left(\frac{\partial u_3}{\partial x_3} \right)^3 \right] \right\rangle}{\left(\left\langle \frac{1}{3} \left[\left(\frac{\partial u_1}{\partial x_1} \right)^2 + \left(\frac{\partial u_2}{\partial x_2} \right)^2 + \left(\frac{\partial u_3}{\partial x_3} \right)^2 \right] \right\rangle \right)^{3/2}}$$

Flatness is defined in the following form:

$$F(t) = \frac{\left\langle \frac{1}{3} \left[\left(\frac{\partial u_1}{\partial x_1} \right)^4 + \left(\frac{\partial u_2}{\partial x_2} \right)^4 + \left(\frac{\partial u_3}{\partial x_3} \right)^4 \right] \right\rangle}{\left(\left\langle \frac{1}{3} \left[\left(\frac{\partial u_1}{\partial x_1} \right)^2 + \left(\frac{\partial u_2}{\partial x_2} \right)^2 + \left(\frac{\partial u_3}{\partial x_3} \right)^2 \right] \right\rangle \right)^2}$$

3.6 Analytical solution of the Taylor-Green vortex problem

For validation of the developed algorithm the classical problem of the 3-D Taylor and Green vortex flow is considered without considering the magnetic field, and the simulated time-dependent turbulence characteristics of this flow were found to be in excellent agreement with the corresponding analytical solution valid for short times.

We duplicate the classical example proposed in [21] in order to validate the numerical simulation of increasing order of accuracy in time and in space $O(\Delta t^2, h^4)$, with efficient

acceleration for sequential algorithm. Starting from a simple incompressible three-dimensional initial condition of the form.

$$\begin{cases} u_1(x_1, x_2, x_3, t = 0) = \cos(ax_1) \sin(ax_2) \sin(ax_3), \\ u_2(x_1, x_2, x_3, t = 0) = -\sin(ax_1) \cos(ax_2) \sin(ax_3), \\ u_3(x_1, x_2, x_3, t = 0) = 0. \end{cases} \quad (19)$$

and assuming periodic conditions in a cubic domain: $0 \leq x_1 \leq 2\pi, 0 \leq x_2 \leq 2\pi, 0 \leq x_3 \leq 2\pi$ with $a = 1$, the three-dimensional filtered Navier-Stokes equation

$$\begin{cases} \frac{\partial u_i}{\partial t} + u_j \frac{\partial u_i}{\partial x_j} = -\frac{1}{\rho} \frac{\partial p}{\partial x_i} + \frac{1}{\text{Re}} \frac{\partial^2 u_i}{\partial x_i \partial x_j}, \\ \frac{\partial u_i}{\partial x_i} = 0. \end{cases} \quad (20)$$

can be solved analytically at small times, using perturbation expansion. In (1) all quantities have been properly normalized by the initial maximum velocity magnitude U_0 in the x_1 or x_2 direction, and $L/2\pi$, where L is the physical domain size, u_i -velocity at $i = 1, 2, 3$, corresponding to x_1, x_2, x_3 directions, $\text{Re} = LU_0/\nu$ is the Reynolds number of flow, U_0 - the characteristic velocity, $T = aU_0t, a = 2\pi/L$. The pressure p has been normalized by ρU_0^2 . Taylor and Green obtained a perturbation expansion of the velocity field, up to $O(t^5)$. The resulting average kinetic energy is:

$$E_k = \frac{U_0^2}{8} u'^2 \quad (21)$$

where

$$\begin{aligned} u'^2 = & 1 - \frac{6T}{\text{Re}} + \frac{18T^2}{\text{Re}^2} - \left(\frac{5}{24} + \frac{36}{\text{Re}^2} \right) \frac{T^3}{\text{Re}} + \left(\frac{5}{2\text{Re}^2} + \frac{54}{\text{Re}^4} \right) T^4 - \\ & - \left(\frac{5}{44.12} + \frac{367}{24\text{Re}^2} + \frac{4.81}{5\text{Re}^4} \right) \frac{T^5}{\text{Re}} + \left(\frac{361}{44.32} + \frac{761}{12\text{Re}^2} + \frac{324}{5\text{Re}^4} \right) \frac{T^6}{\text{Re}^2}. \end{aligned} \quad (22)$$

The dissipation rate is written in the following form:

$$W = \mu \frac{3U_0^2 a^2}{4} W' \quad (23)$$

where

$$\begin{aligned} W' = & 1 - \frac{6T}{\text{Re}} + \left(\frac{5}{48} + \frac{18T^2}{\text{Re}^2} \right) T^2 - \left(\frac{5}{3} + \frac{36}{\text{Re}^2} \right) \frac{T^3}{\text{Re}} + \\ & + \left(\frac{50}{99.64} + \frac{1835}{9.16\text{Re}^2} + \frac{54}{\text{Re}^4} \right) T^4 - \left(\frac{361}{44.32} + \frac{761}{12\text{Re}^2} + \frac{324}{5\text{Re}^4} \right) \frac{T^5}{\text{Re}}. \end{aligned} \quad (24)$$

Simulation at different Reynolds numbers was compared with the analytical solution of the Taylor-Green vortex problem from the point of view of: the average kinetic energy and the average dissipation rate of the turbulent flow. Figure 2 compares the average turbulent kinetic energy obtained in this paper with the analytical solution of the Taylor-Green vortex problem for different Reynolds numbers. The results obtained by analytical solution of short-time theory of TG, spectral methods at 256^3 grid resolution and hybrid finite difference method at 128^3 grid resolution show a satisfactory agreement till $T = 3$ at $Re = 100$, and till $T = 4$ at $Re = 300$ and $Re = 600$ for the average turbulent kinetic energy. The error between analytical and numerical solutions for the average kinetic energy was defined as: $Error(E_k) = |E_k^{HFD} - E_k^{TG}| = 10^{-4}$.

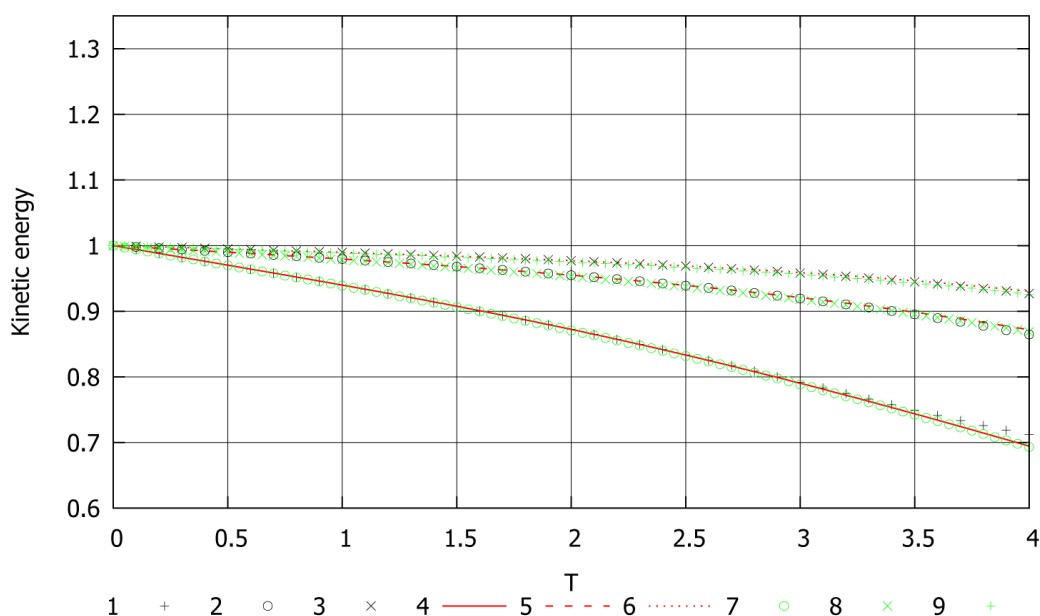


Figure 2: Comparative results of modeling the evolution of the average kinetic energy in time, spectral and hybrid methods of modeling the Taylor-Green vortex of: TG short-time theory at: 1) $Re=100$; 2) $Re=300$; 3) $Re=600$; Spectral method, 256^3 at: 4) $Re=100$; 5) $Re=300$; 6) $Re=600$; HFD method at: 7) $Re=100$; 8) $Re=300$; 9) $Re=600$.

Figure 3 compares the results of average rate of dissipation of the turbulence decay with respect to time of the numerical simulation, and the analytical solution of the Taylor-Green vortex problem at different Reynolds number. It can be seen from Figure 3 that the short-term theoretical results and numerical simulation results are in good agreement till $T = 2.5$ for $Re = 100$, and $T = 2$ for $Re = 300$; $Re = 600$. It is difficult to compare the analytical solution with numerical simulation, since the analytical solution valid only for short-term time, and the numerical solution can provide good results for long term, so it is worthwhile to compare simulation results of spectral method and HFD method for long term. The rate of dissipation increases sharply due to the formation of small-scale flow structures and reaches a maximum at $T = 3$, for short time theory of TG at $Re = 100$, and at $T = 4$ for other case, and then the rate of dissipation shows a decrease in the tendency for result of analytical solution of TG at $Re = 100$ because of the decrease in the total Reynolds number of the

stream. In the simulation results, the error between analytical and numerical solutions for the average dissipation rate is: $Error(\epsilon) = |\epsilon^{HFDM} - \epsilon^{TG}| = 10^{-2}$.

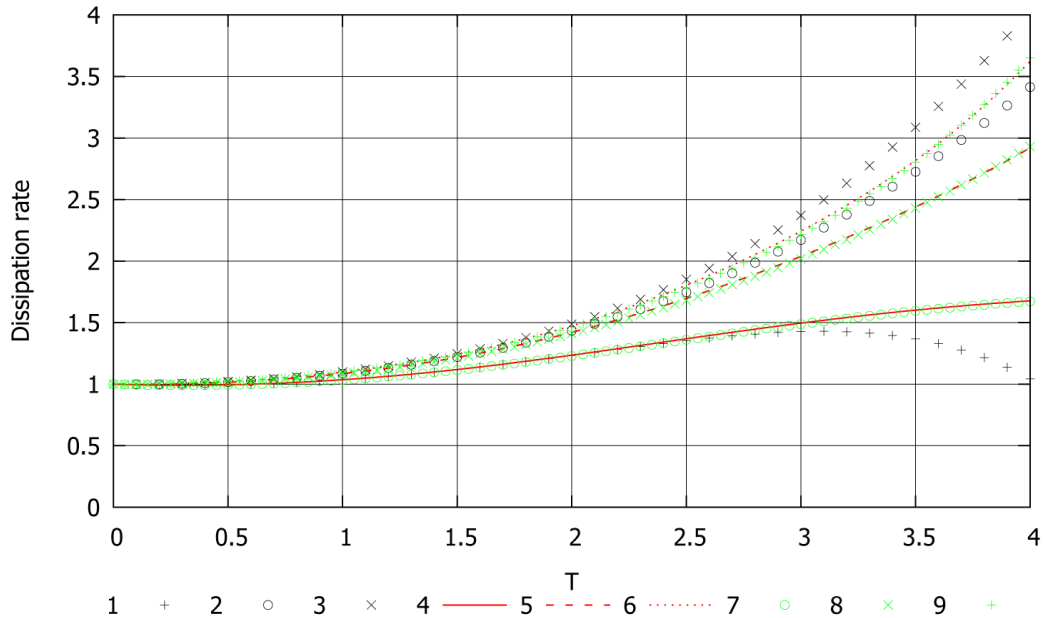


Figure 3: Comparative results of modeling the evolution of the average rate of dissipation of the decay of turbulence in time, the spectral and hybrid methods of modeling the Taylor-Green vortexof: TG short-time theory at: 1) $Re=100$; 2) $Re=300$; 3) $Re=600$; Spectral method, 256^3 at: 4) $Re=100$; 5) $Re=300$; 6) $Re=600$; HFD method at: 7) $Re=100$; 8) $Re=300$; 9) $Re=600$.

Figure 4 shows that with the increase in the resolution of the computational grid, the results of skewness of the turbulence of hybrid method tends gently to the exponential results of the pseudospectral method for the computational grid $256 \times 256 \times 256$.

Figure 5 shows the results of modeling the evolution of flatness, spectral and hybrid methods for modeling the Taylor-Green vortex at $Re = 300$.

4 Results and discussion

Numerical model allows to describe the homogeneous magnetohydrodynamic turbulence decay based on large eddy simulation. For this task, the kinematic viscosity $\nu = 10^{-4}$ was taken constant and the magnetic viscosity were set in the range of $\nu_m = 10^{-3} \div 10^{-4}$. The characteristic values of the velocity, length, magnetic field strength were taken equal to: $U_{CH} = 1$, $L_{CH} = 1$, $H_{CH} = 1$ respectively. Reynolds number is $Re = 10^4$, the magnetic Reynolds number varied depending on the magnetic viscosity coefficient. The Alfvén number characterizing the motion of conductive fluid for various numbers of magnetic Reynolds: $A = Ha^2/Re_m$, where Hartmann number is $Ha = 1$. For the calculations used grid size $128 \times 128 \times 128$. The time step was taken equal $\Delta\tau = 0.001$.

As result of simulation at different magnetic Reynolds numbers were obtained the following turbulence characteristics: integral scale and Taylor scale.

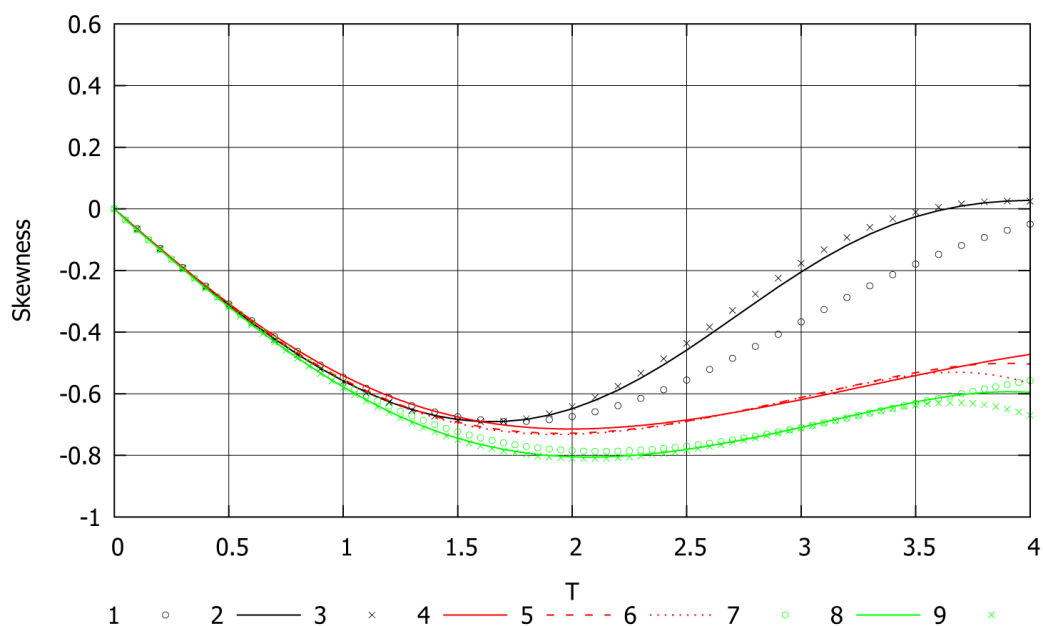


Figure 4: Comparison of the results of modeling the evolution of skewness, spectral and hybrid methods for modeling the Taylor-Green vortex of: TG short-time theory at: 1) $Re=100$; 2) $Re=300$; 3) $Re=600$; Spectral method, 256^3 at: 4) $Re=100$; 5) $Re=300$; 6) $Re=600$; HFD method at: 7) $Re=100$; 8) $Re=300$; 9) $Re=600$.

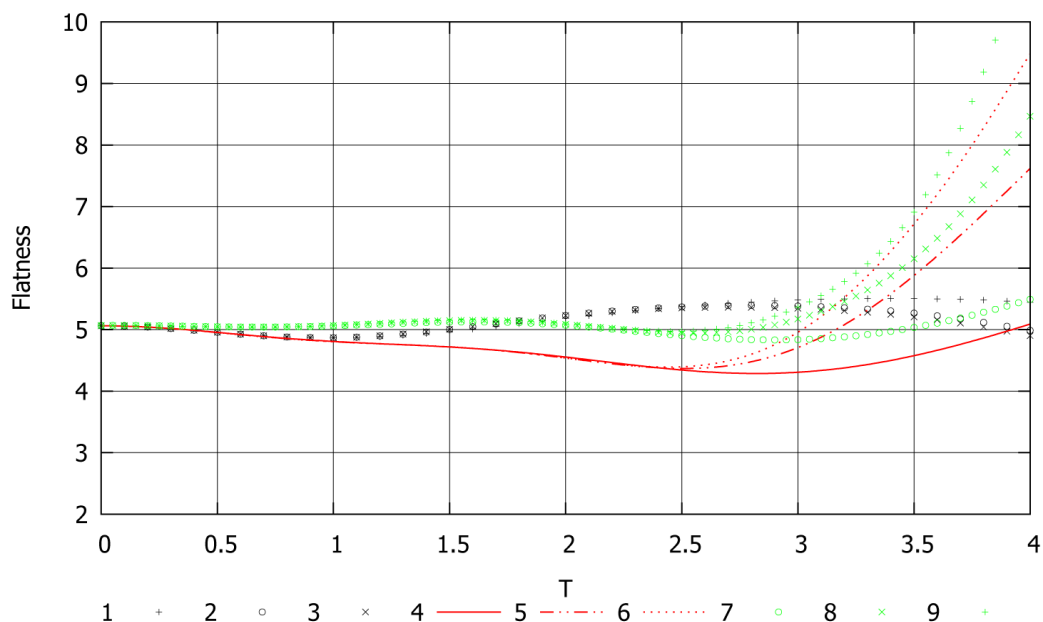


Figure 5: Comparison of the results of modeling the evolution of flatness, spectral and hybrid methods for modeling the Taylor-Green vortex of: TG short-time theory at: 1) $Re=100$; 2) $Re=300$; 3) $Re=600$; Spectral method, 256^3 at: 4) $Re=100$; 5) $Re=300$; 6) $Re=600$; HFD method at: 7) $Re=100$; 8) $Re=300$; 9) $Re=600$.

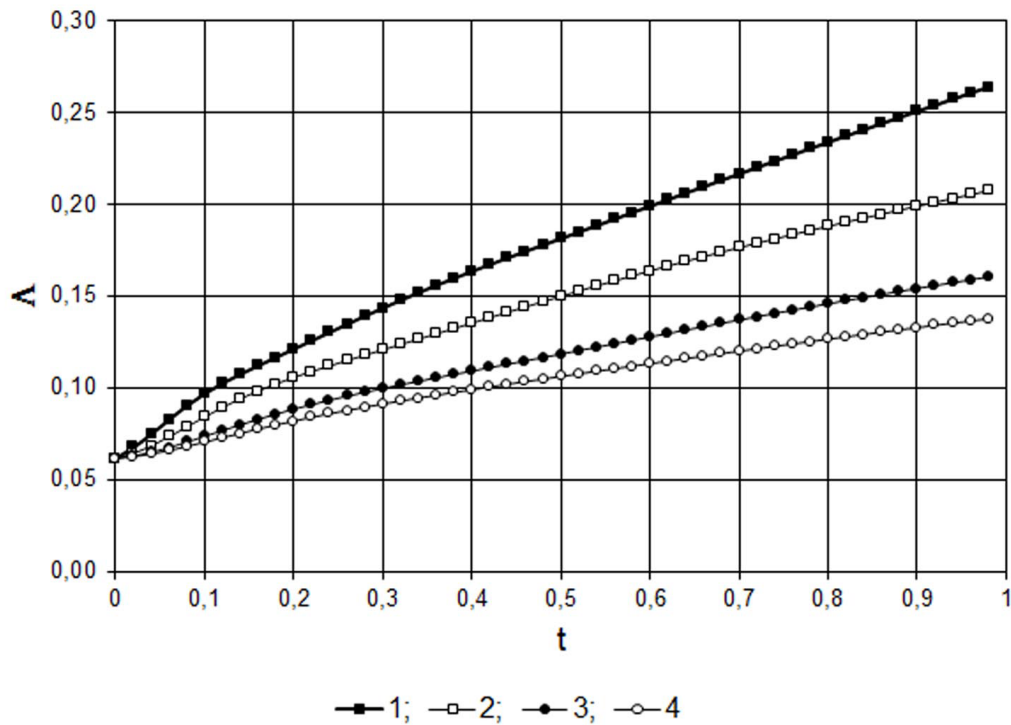


Figure 6: Change of the integral turbulence scale calculated at different magnetic Reynolds numbers: 1) $Re_m = 10^3$; 2) $Re_m = 2 \cdot 10^3$; 3) $Re_m = 5 \cdot 10^3$; 4) $Re_m = 10^4$.

According to semi-empirical theory of turbulence integral scale should grow with time. The results presented in Figure 6 illustrates the effect of magnetic viscosity on the internal structure of the MHD turbulence. Variation of the coefficient of magnetic viscosity leads to a proportional change in the integral scale. Figure 6 shows that the size of large eddies rapidly increases at small number of magnetic Reynolds $Re_m = 10^3$, than in the case, when $Re_m = 10^4$ which leads to fast energy dissipation.

Figure 7 shows the change in the micro scale - calculated at different numbers of magnetic Reynolds 1) $Re_m = 10^3$; 2) $Re_m = 2 \cdot 10^3$; 3) $Re_m = 5 \cdot 10^3$; 4) $Re_m = 10^4$. Figure 7 shows the change of the Taylor microscale at different magnetic Reynolds numbers. It can be seen that in the case $Re_m = 10^3$ when the magnetic viscosity coefficient is large then the dissipation rate increases. In the case when the magnetic viscosity coefficient is smaller then the scale gradually increases, and the small scale structure of the turbulence tends to slowly isotropy. This also indicates that with small numbers Re_m the decay of isotropic turbulence occurs faster than in the case when Re_m is high.

From the figures it is seen that in the case of high medium conductivity at $Re_m = 10^3$ the frictional force increases and the flow rate is reduced faster than, at $Re_m = 10^4$, that corresponds to the low conductivity of the medium, in this version, the frictional force have minimal impact on the flow velocity. Based on the study of the results determined that the first part of the turbulent kinetic energy is used for turbulent mixing, the second part - at creating magnetic field and the third part - on the forces of resistance between the components of the velocity and magnetic tension.

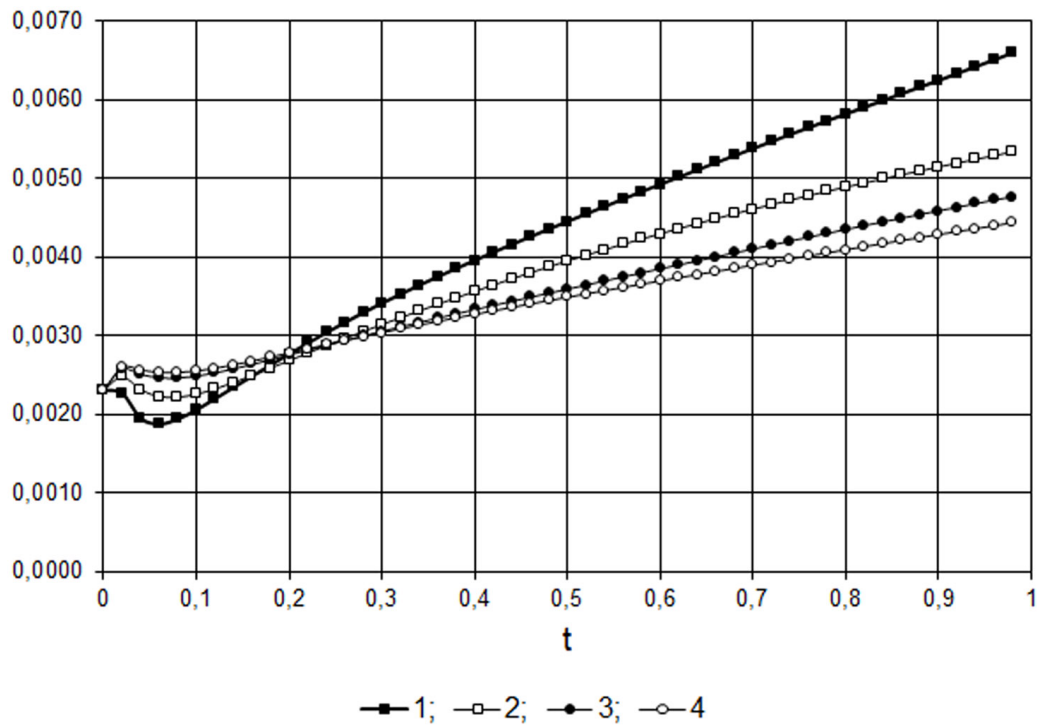


Figure 7: Change of Taylor-scale calculated at different magnetic Reynolds numbers: 1) $Re_m = 10^3$; 2) $Re_m = 2 \cdot 10^3$; 3) $Re_m = 5 \cdot 10^3$; 4) $Re_m = 10^4$.

5 Conclusion

Based on the method large-eddy simulation was produced the numerical modelling of influence magnetic viscosity to decay of magnetohydrodynamic turbulence, analyzing simulation results it is possible to make the following conclusion: the magnetic viscosity of the flow has a significant influence on the MHD turbulence. Obtained results allow sufficiently accurately calculate the change characteristics of magnetohydrodynamic turbulence over time at different magnetic Reynolds numbers. To simulate the turbulence energy degeneration, a numerical algorithm for solving the unsteady three-dimensional Navier-Stokes equations based on the hybrid method was developed. The numerical algorithm is a hybrid method combining finite difference and spectral methods. It is also computationally efficient. The finite-difference method combined with the cyclic Penta-diagonal matrix for the solution of the Navier-Stokes equations allowed to achieve the accuracy of the fourth order in space and the accuracy of the second order in time. The spectral method for solving the Poisson equation has a high computational efficiency by using a fast Fourier transform library.

To check the adequacy of the developed algorithm, the classical Taylor and green problem with the same initial flow conditions, for modeling the degeneracy of the kinetic energy of the flow and the time evolution of viscous dissipation is considered. Average normalized errors between analytical and numerical solutions for mean kinetic energy and mean dissipation rate were established as $Error(E_k) = |E_k^{FDM} - E_k^{TG}| = 10^{-4}$, $Error(\epsilon) = |\epsilon^{FDM} - \epsilon^{TG}| = 10^{-2}$, respectively. Thus, the results of numerical simulation of turbulence characteristics show very

good agreements with the analytical solution. Thus, the numerical algorithm was developed for solving unsteady three-dimensional magnetohydrodynamic equations, and makes it possible to simulate the MHD turbulence decay at different magnetic Reynolds numbers.

6 Acknowledgment

The work was supported by grant financing of scientific and technical programs and projects by the Ministry of Education and Science of the Republic of Kazakhstan (grant «Development of a three-dimensional mathematical model of the effect of electron concentration on the dynamics of changes in the inhomogeneities of the ionosphere E-layer in the dependence of solar radiation intensity», 2018-2020 years)

References

- [1] Abdibekova A., Zhakebayev D., Abdigaliyeva A. and Zhubat K., "Modelling of turbulence energy decay based on hybrid methods," *Engineering Computations* 35(5), (2018):1965-77.
- [2] Batchelor G. K. "On the spontaneous magnetic field in a conducting liquid in turbulent motion," *Proc. Roy. Soc. A* 201. 16(1950): 405-16.
- [3] Batchelor G. K., *The theory of homogeneous turbulence* (Cambridge University Press: 1953)
- [4] Batista M., "A Method for Solving Cyclic Block Penta-diagonal Systems of Linear Equations," *ArXiv*, March 6, 2008. Accessed March 14, 2008. <http://arxiv.org/abs/0803.0874>.
- [5] Brachet M.E. , Meiron D. I., Orszag S. A., Nickel B. G., Morf R.H. and Frisch U., "Small-scale structure of the Taylor-Green vortex" *Fluid Mechanics* 130(1983): 411-52.
- [6] Brachet M.E., "Direct simulation of three - dimensional turbulence in the Taylor - Green vortex," *Fluid Dynamics Research* 8(1991): 1-8.
- [7] Burattini P., Zikanov O. and Knaepen B., "Decay of magnetohydrodynamic turbulence at low magnetic Reynolds number" *Fluid Mechanics* 657(2010): 502-38.
- [8] DeBonis J.R., "Solutions of the Taylor-Green vortex problem using high - resolution explicit finite difference methods" (paper presented at 51st AIAA Aerospace Sciences Meeting including the New Horizons Forum and Aerospace Exposition, Dallas, Texas, January 07–10, 2013).
- [9] Hossain M., "Inverse energy cascades in three dimensional turbulence," *Physics of Fluids B: Plasma Physics* 3(2)(1991): 511-14.
- [10] Frisch U., *Turbulence. The legacy of A.N. Kolmogorov* (Cambridge University Press: 1995)
- [11] Ievlev V. M., *The method of fractional steps for solution of problems of mathematical physics* (Moscow: Science Nauka: 1975)
- [12] Kampanis N.A. and Ekaterinaris J.A., "A staggered grid, high-order accurate method for the incompressible Navier-Stokes equations," *Computational Physics* 215(2006): 589-613.
- [13] Kim J. and Moin P., "Application of a fractional - step method to incompressible Navier- Stokes equations," *Computational Physics* 59(1985): 308-23.
- [14] Knaepen B., Kassinos S. and Carati D., "Magnetohydrodynamic turbulence at moderate magnetic Reynolds number" *Fluid Mechanics* 513(3)(2004): 199-220.
- [15] Kolmogorov A. N., "Local structure of turbulence in an incompressible fluid at very high Reynolds numbers" *Doklady Akademii Nauk USSR* 30(1941): 299-303.
- [16] Moffatt H. K., "On the suppression of turbulence by a uniform magnetic field," *Fluid Mechanics* 28(1967): 571-592.
- [17] Monin A. C., Yaglom A. M., *Statistical fluid mechanics* (Cambridge: MIT Press: 1975)

-
- [18] Navon M., "Pent: A periodic pentadiagonal systems solver," *Communications in applied numerical methods* 3(1987): 63-9.
- [19] Schumann U., "Numerical simulation of the transition from three- to two-dimensional turbulence under a uniform magnetic field," *Fluid Mechanics* 74(1976):31-58.
- [20] Sirovich L., Smith L., Yakhot V., "Energy spectrum of homogeneous and isotropic turbulence in far dissipation range," *Physical Review Letters* 72(3)(1994): 344-47.
- [21] Taylor G.I. and Green A.E., "Mechanism of production of small eddies from large ones," *Proceedings of the royal society, Mathematics and physical sciences* 158(895)(1937): 499-521.
- [22] Vorobev A., Zikanov O., Davidson P. and Knaepen B., "Anisotropy of magnetohydrodynamic turbulence at low magnetic Reynolds number," *Physics of Fluids* 17(2005): 125105-1-125105-12.
- [23] Zhakebayev D., Zhumagulov B. and Abdibekova A., "The decay of MHD turbulence depending on the conductive properties of the environment," *Magnetohydrodynamics* 50(2)(2014): 121-38.
- [24] Zikanov O. and Thess A., "Direct numerical simulation of forced MHD turbulence at low magnetic Reynolds number," *Fluid Mechanics* 358(1998): 299-333.